Electrothermal Coupling in Floating Photovoltaic Systems: A Modified Shockley Framework for Performance Enhancement

M. Arucu*

Department of Computer Technologies, Bandırma Onyedi Eylül University, Altay Mh., Gönen, 10900 Balikesir, Türkiye

Received: 06.04.2026 & Accepted: 15.06.2026

Doi: 10.12693/APhysPolA.149.157 *e-mail: marucu@bandirma.edu.tr

Floating photovoltaic systems are attracting increasing attention due to their enhanced thermal regulation and improved energy yield compared to land-based installations; however, accurately capturing their coupled thermal–electrical behavior under realistic environmental conditions remains a key challenge. In this study, a physics-based electrothermal framework is developed by extending the classical Shockley diode equation to explicitly incorporate water-assisted cooling effects. A floating photovoltaic-specific thermal correction is introduced to directly link environmental variables — including irradiance, ambient temperature, water temperature, and wind speed — to temperature-dependent electrical parameters. The results show that reduced operating temperatures significantly suppress the exponential increase in diode saturation current, leading to improved voltage retention and enhanced maximum power output. Comparative I–V and P–V analyses indicate that the performance gain of floating photovoltaic systems is predominantly voltage-driven, with predicted power improvements of $\approx$ 3–8% under typical operating conditions. Sensitivity and Monte Carlo analyses further demonstrate the robustness of the floating photovoltaic system advantages and highlight the dominant influence of water temperature and wind speed on system performance. The proposed framework provides a compact, physically interpretable, and computationally efficient tool for floating photovoltaic performance analysis, offering practical insights for system design and optimization.

topics: floating photovoltaics (FPV), modified Shockley model, electrothermal coupling, photovoltaic performance

1. Introduction

The rapid increase in global energy demand, together with the urgent need to mitigate environmental degradation, has accelerated the deployment of renewable energy technologies, among which solar photovoltaics (PV) have emerged as a key solution [1, 2]. Although conventional land-based photovoltaic systems are widely implemented, their large-scale expansion is often limited by land availability, environmental impact, and thermal performance limitations. In this context, floating photovoltaic (FPV) systems have gained significant attention as an alternative deployment strategy, offering advantages such as reduced land use, mitigation of water evaporation, and suppression of algal growth [3–6].

One of the primary factors contributing to the superior performance of FPV systems is the cooling effect of the underlying water body [7–9]. Enhanced convective and conductive heat transfer mechanisms lower the operating temperature of photovoltaic modules, leading to improved electrical efficiency and reduced thermal degradation [10, 11]. Previous studies have reported efficiency improvements ranging from 1.5% to 2.0%, with even higher gains achievable under active cooling conditions [12]. These findings highlight the critical role of thermal regulation in determining photovoltaic performance and emphasize the need for accurate electrothermal modeling approaches. In addition, lower operating temperatures can result in increases in energy yields of up to 15%, further highlighting the importance of thermal effects in photovoltaic performance [13].

Effective thermal management is therefore a critical factor in both conventional and floating photovoltaic systems [14]. Elevated operating temperatures not only reduce conversion efficiency but also accelerate material degradation, thereby limiting the lifetime of the system and the energy yield [15, 16]. In FPV systems, the surrounding water body acts as a natural heat sink, mitigating temperature-induced losses and improving overall system performance [17, 18]. This thermal regulation directly affects the current–voltage characteristics of photovoltaic modules by modifying temperature-dependent parameters in the Shockley diode equation, particularly the reverse saturation current and the ideality factor [19]. Consequently, accurate modeling of the electrothermal interaction is essential for reliable performance prediction and system optimization.

In recent years, increasing attention has been directed towards integrating thermal and electrical processes within unified modeling frameworks to enhance the accuracy of photovoltaic system performance predictions [20–22]. However, conventional approaches often treat temperature as an external or empirical parameter, which limits their ability to capture the intrinsic feedback mechanisms between environmental conditions and the electrical response. This limitation becomes particularly critical in FPV systems, where continuous interaction between the module, the surface of the water, and the ambient environment dynamically governs heat dissipation and operating temperature [23, 24].

Despite these advances, there is still a lack of compact and physically interpretable models that simultaneously incorporate diode-level physics and FPV-specific thermal effects. To address this gap, the present study develops a physics-based electrothermal modeling framework by extending the classical Shockley diode equation to explicitly incorporate water-assisted cooling mechanisms [25, 26]. The proposed model introduces an explicit electrothermal coupling formulation that directly links environmental variables — including irradiance, ambient temperature, water temperature, and wind speed — to temperature-dependent electrical parameters, thereby enabling a more realistic representation of FPV system behavior.

The main contributions of this study can be summarized as follows:

- A modified Shockley-based electrothermal model is formulated for FPV systems by explicitly incorporating water-assisted thermal regulation.
- The influence of floating-specific environmental conditions on key electrical parameters, including open-circuit voltage, short-circuit current, and maximum power point, is systematically analyzed.
- A comparative framework between floating and land-based photovoltaic systems is established to quantify performance differences.
- A set of physics-based performance indicators and visualization tools is introduced to support simulation-based and experimental validation studies.

Overall, this work provides a physically grounded and computationally efficient framework for understanding and optimizing the performance of FPV systems, offering new insights into the electrothermal mechanisms governing energy conversion in floating photovoltaic installations.

2. Theoretical framework: Shockley diode equation

The Shockley diode equation constitutes the fundamental analytical basis for describing the current–voltage behavior of p–n junction devices and is therefore widely used in photovoltaic modeling. Under illuminated conditions, the electrical response of a solar cell is commonly represented by the modified Shockley formulation, referred to as the single-diode model, which incorporates parasitic resistances and temperature-dependent semiconductor behavior. In photovoltaic systems, this framework is especially important because the output current, voltage, and power are strongly governed by environmental variables, most notably solar irradiance and cell temperature [27, 28].

In practical operation, an increase in cell temperature generally reduces open-circuit voltage and only slightly increases short-circuit current, resulting in a net decrease in power conversion efficiency [29, 30]. This thermal sensitivity arises primarily from the exponential increase in the diode saturation current with temperature, together with the carrier transport and temperature-dependent recombination processes [31]. Therefore, accurate thermal representation is essential to predict reliable photovoltaic performance, particularly in FPV systems, where the surrounding water body modifies the heat-transfer balance and introduces an additional cooling pathway [32].

Accordingly, the conventional Shockley framework is extended here to incorporate FPV-specific thermal regulation effects. The following subsections establish the governing electrothermal equations, define the temperature-dependent electrical parameters, and formulate the floating-specific correction required to describe photovoltaic behavior under aquatic operating conditions.

2.1. Single- and two-diode representation of photovoltaic cells

Under illuminated conditions, the electrical behavior of a photovoltaic device is commonly described by the modified Shockley single-diode model, expressed as

$$I = I_{\mathrm{ph}} - I_0 \left[\exp\left(\frac{q(V+IR_s)}{n\,k_{\mathrm{B}}T_c}\right) - 1\right] - \frac{V+IR_s}{R_{sh}}, \tag{1}$$

where I and V denote the output current and terminal voltage, respectively, I_{ph} is the photocurrent,

I_0 is the reverse saturation current, R_s and R_{sh} are the resistances of the series and shunt, respectively, n is the ideality factor, q is the electron charge, k_B is the Boltzmann constant, and T_c is the cell temperature. This formulation captures the combined effects of photogeneration, recombination, and resistive losses, with temperature directly influencing the exponential diode term.

Although the single-diode model provides a compact and widely adopted representation, it may not fully capture recombination mechanisms under non-ideal conditions. To improve accuracy, particularly under varying irradiance and temperature, the two-diode model can be employed as

$$I = I_\mathrm{ph} - I_{01}\left[\exp\left(\frac{q(V+IR_s)}{n_1\, k_\mathrm{B} T_c}\right) - 1\right] - I_{02}\left[\exp\left(\frac{q(V+IR_s)}{n_2\, k_\mathrm{B} T_c}\right) - 1\right] - \frac{V+IR_s}{R_{sh}}, \qquad (2)$$

where I_{01} and I_{02} represent the saturation currents associated with diffusion and recombination processes, respectively, and n_1 and n_2 are their corresponding ideality factors. This extended formulation enables an improved representation of non-ideal carrier recombination and is particularly relevant for systems operating under dynamically varying environmental conditions, such as floating photovoltaic installations. Importantly, both formulations remain strongly temperature-dependent, which is central to the electrothermal analysis developed in this study.

2.2. Temperature-dependent electrical parameters

The electrical response of photovoltaic devices is governed by a set of parameters that exhibit a strong dependence on both irradiance and temperature. Among these, the photocurrent and the diode saturation current play a central role in determining the current–voltage characteristics and overall device performance.

The photocurrent is primarily controlled by the incident solar irradiance and exhibits a weak but non-negligible temperature dependence, which can be expressed as

$$I_\mathrm{ph} = \Big[I_\mathrm{sc,ref} + \alpha_I\big(T_c - T_\mathrm{ref}\big)\Big]\frac{G}{G_\mathrm{ref}}, \qquad (3)$$

where $I_\mathrm{sc,ref}$ is the short-circuit current under reference conditions, α_I is the coefficient of current temperature, G is the incident irradiance, G_ref is the reference irradiance, and T_ref is the reference temperature. This relation reflects the near-linear scaling of the photocurrent with irradiance and its relatively weak thermal sensitivity.

In contrast, the reverse saturation current exhibits a strong exponential dependence on temperature and is given by

$$I_0(T_c) = I_\mathrm{0,ref}\left(\frac{T_c}{T_\mathrm{ref}}\right)^3 \exp\left[\frac{qE_g}{n\, k_\mathrm{B}}\left(\frac{1}{T_\mathrm{ref}} - \frac{1}{T_c}\right)\right], \qquad (4)$$

where $I_\mathrm{0,ref}$ is the saturation current under reference conditions, and E_g is the semiconductor band-gap energy. The exponential increase in I_0 with temperature constitutes the dominant mechanism responsible for voltage degradation in photovoltaic devices.

As a consequence, the open-circuit voltage can be approximated as

$$V_\mathrm{oc} \approx \frac{n\, k_\mathrm{B} T_c}{q}\ln\left(\frac{I_\mathrm{ph}}{I_0} + 1\right), \qquad (5)$$

highlighting the strong sensitivity of voltage to temperature through the saturation current. Although the short-circuit current increases only marginally with temperature, the rapid growth of I_0 leads to a pronounced reduction in V_oc, thus limiting the maximum achievable power.

This asymmetry in temperature sensitivity establishes the fundamental electrothermal behavior of photovoltaic devices: performance degradation at elevated temperatures is primarily voltage-driven. In floating photovoltaic systems, where water-assisted cooling reduces operating temperature, this mechanism directly translates into improved voltage retention and enhanced power conversion efficiency. Importantly, this temperature-driven voltage limitation forms the physical basis for the performance advantage observed in floating photovoltaic systems.

2.3. FPV-specific thermal correction

A defining characteristic of FPV systems is the presence of a water body acting as an additional thermal sink, which fundamentally alters the heat-transfer balance of the photovoltaic module. In contrast to land-based systems, where heat dissipation is governed primarily by ambient air and wind-driven convection, FPV installations experience enhanced thermal regulation due to the combined effects of water-assisted cooling and convective heat exchange.

To capture this behavior within a physically consistent framework, cell temperature is expressed as

$$T_c = T_a + \frac{G}{U}, \qquad (6)$$

where T_a is the ambient temperature and U is the effective heat-loss coefficient. Although this formulation is commonly used for conventional photovoltaic systems, it does not account for the additional thermal interactions introduced by floating configurations.

In this study, the heat-loss coefficient is extended to incorporate FPV-specific environmental effects as

$$U_{\mathrm{FPV}} = U_0 + U_1\,v + U_2\,(T_a - T_w), \tag{7}$$

where U_0 represents the baseline heat-loss coefficient, $U_1 v$ accounts for wind-driven convective enhancement, and $U_2\,(T_a - T_w)$ introduces a water-cooling term that explicitly captures the thermal interaction between the module and the underlying temperature of the water body, T_w. This additional term constitutes the key modification that differentiates FPV systems from conventional land-based models.

Substituting (7) into (6), the FPV-adjusted cell temperature becomes

$$T_c^{\mathrm{FPV}} = T_a + \frac{G}{U_0 + U_1 v + U_2 (T_a - T_w)}. \tag{8}$$

This formulation establishes a direct coupling between environmental conditions and the internal thermal state of the PV device. In particular, lower water temperatures and higher wind speeds increase the effective heat-loss coefficient, thus reducing the operating temperature of the module.

The novelty of the proposed approach lies in embedding this FPV-specific thermal correction directly into the temperature-dependent electrical relations of the Shockley model. By doing so, the electrothermal response of the system becomes explicitly governed by aquatic environmental parameters, enabling a physically interpretable link between water-assisted cooling and photovoltaic performance. As T_c^{FPV} directly enters the diode current, saturation current, and voltage expressions, the entire I–V and P–V characteristics of the system are shifted toward a more favorable operating regime, characterized by improved voltage retention and power output.

This electrothermal coupling mechanism provides the fundamental basis for the enhanced performance observed in floating photovoltaic systems.

2.4. Modified Shockley framework for FPV applications

By introducing the FPV-corrected cell temperature into the temperature-dependent electrical relations, the modified current equation for floating photovoltaic systems can be written as

$$I_{\mathrm{FPV}} = I_{\mathrm{ph}}(G, T_c^{\mathrm{FPV}}) - I_0(T_c^{\mathrm{FPV}}) \left[\exp\left(\frac{q\,(V + I_{\mathrm{FPV}}\,R_s)}{n\,k_{\mathrm{B}} T_c^{\mathrm{FPV}}} \right) - 1 \right] - \frac{V + I_{\mathrm{FPV}} R_s}{R_{sh}}. \tag{9}$$

This formulation provides a compact but physically meaningful representation of the electrothermal behavior of FPV systems. It shows that water-assisted cooling modifies the diode current indirectly through its effect on cell temperature, preserves a higher open-circuit voltage, and shifts the operating point toward improved electrical efficiency.

If a more detailed recombination analysis is required, the same thermal correction can be incorporated into the two-diode framework of (2). In that case, the FPV-adjusted temperature governs both diode branches and enables an improved representation of non-ideal carrier recombination under dynamic aquatic operating conditions.

To clarify the modification introduced in the present framework, the classical Shockley-based single-diode formulation has been modified at three levels. First, the cell temperature is no longer treated as an externally prescribed constant, but is computed from an FPV-specific thermal balance that includes ambient temperature, water temperature, irradiance, and wind speed. Second, the resulting FPV-adjusted temperature T_c^{FPV} is propagated into the temperature-dependent electrical quantities, particularly the photocurrent $I_{\mathrm{ph}}(G, T_c^{\mathrm{FPV}})$ and the diode saturation current $I_0(T_c^{\mathrm{FPV}})$. Third, the modified temperature-dependent parameters are inserted into the Shockley equation, thereby allowing water-assisted cooling to directly influence the I–V and P–V characteristics of the module.

The newly introduced FPV-specific parameters are the baseline floating heat-loss coefficient U_0, the wind-dependent heat-loss coefficient U_1, and the water-cooling interaction coefficient U_2. These coefficients determine the effective heat-loss coefficient U_{FPV} and therefore control the FPV-adjusted cell temperature. In the present numerical implementation, representative values were adopted: $U_0 = 26$ W/(m^2 K), $U_1 = 5.5$ W/(m^2 K)/(m/s), and $U_2 = 0.9$ W/(m^2 K^2). These values were selected to represent enhanced thermal dissipation in floating configurations relative to land-based systems and were calibrated against reference photovoltaic parameters and literature-reported thermal coefficients. Sensitivity analyses were then performed to evaluate the effect of parameter variation on the predicted FPV performance.

Overall, the modified Shockley framework developed here establishes a direct connection between floating-system thermal conditions and photovoltaic electrical response. This theoretical basis provides a consistent foundation for interpreting I–V and P–V characteristics and for the comparative analyses presented in the subsequent methodology and results sections.

TABLE I

Reference values used in the modified Shockley-based FPV electrothermal model.

Parameter	Symbol	Value	Unit
Reference irradiance	G_{ref}	1000	W/m^2
Reference temperature	T_{ref}	25	°C
Reference short-circuit current	$I_{\text{sc,ref}}$	9.50	A
Reference open-circuit voltage	$V_{\text{oc,ref}}$	37.5	V
Current temperature coefficient	α_I	4.75×10^{-3}	A/K
Ideality factor	n	1.30	–
Series resistance	R_s	0.35	Ω
Shunt resistance	R_{sh}	500	Ω
Band-gap energy	E_g	1.12	eV
Land baseline heat-loss coefficient	$U_{0,\text{land}}$	20.0	W/(m^2 K)
Land wind coefficient	$U_{1,\text{land}}$	4.0	W/(m^2 K)/(m/s)
FPV baseline heat-loss coefficient	U_0	26.0	W/(m^2 K)
FPV wind coefficient	U_1	5.5	W/(m^2 K)/(m/s)
Water-cooling coefficient	U_2	0.9	W/(m^2 K^2)
Reference ambient temperature	T_a	30	°C
Reference water temperature	T_w	22	°C
Reference wind speed	v	2.5	m/s

3. Methodology

This section presents the integrated electrothermal modeling framework developed to evaluate the performance of FPV systems. The methodology combines a modified Shockley diode formulation with an FPV-specific thermal model, enabling direct coupling between environmental conditions and the electrical response of the photovoltaic module.

The proposed approach is based on both single- and two-diode representations, allowing for accurate characterization of carrier transport and recombination processes under varying irradiance and temperature conditions. Particular emphasis is placed on FPV-specific thermal mechanisms, including water-assisted cooling, wind-driven convection, and ambient–water thermal interaction, all of which govern the operating cell temperature and, consequently, influence the electrical behavior of the system.

The model takes environmental variables, i.e., solar irradiance (G), ambient temperature (T_a), water temperature (T_w), and wind speed (v), as primary inputs. These parameters are used to estimate the cell temperature adjusted for FPV using (8), which explicitly accounts for the increased heat dissipation in floating configurations. The resulting temperature is then incorporated into temperature-dependent electrical parameters, including the photocurrent and diode saturation current, ensuring a consistent and physically grounded evaluation of the I–V and P–V characteristics.

The nonlinear diode equations are solved numerically using iterative techniques to determine the operating current at each voltage point. From the resulting I–V curves, key performance indicators, such as open-circuit voltage (V_{oc}), short-circuit current (I_{sc}), maximum power ($P_{\max}$), and conversion efficiency (η), are extracted.

To ensure physical consistency, model parameters are calibrated using reference photovoltaic data and temperature coefficients reported in the literature [33–36]. In addition to steady-state analysis, environmental variability is incorporated through parametric sweeps and stochastic perturbations, enabling the representation of transient effects such as wave-induced motion and short-term irradiance fluctuations.

The numerical values adopted for the reference simulations are shown in Table I. These values define the baseline module and thermal and environmental conditions used to generate the comparative I–V, P–V, sensitivity, and uncertainty results.

In general, the proposed framework provides a compact yet physically interpretable methodology to evaluate FPV systems under realistic environmental conditions. By explicitly linking thermal regulation to electrical response, the model enables systematic comparison between floating and land-based photovoltaic systems and supports performance-oriented design and optimization.

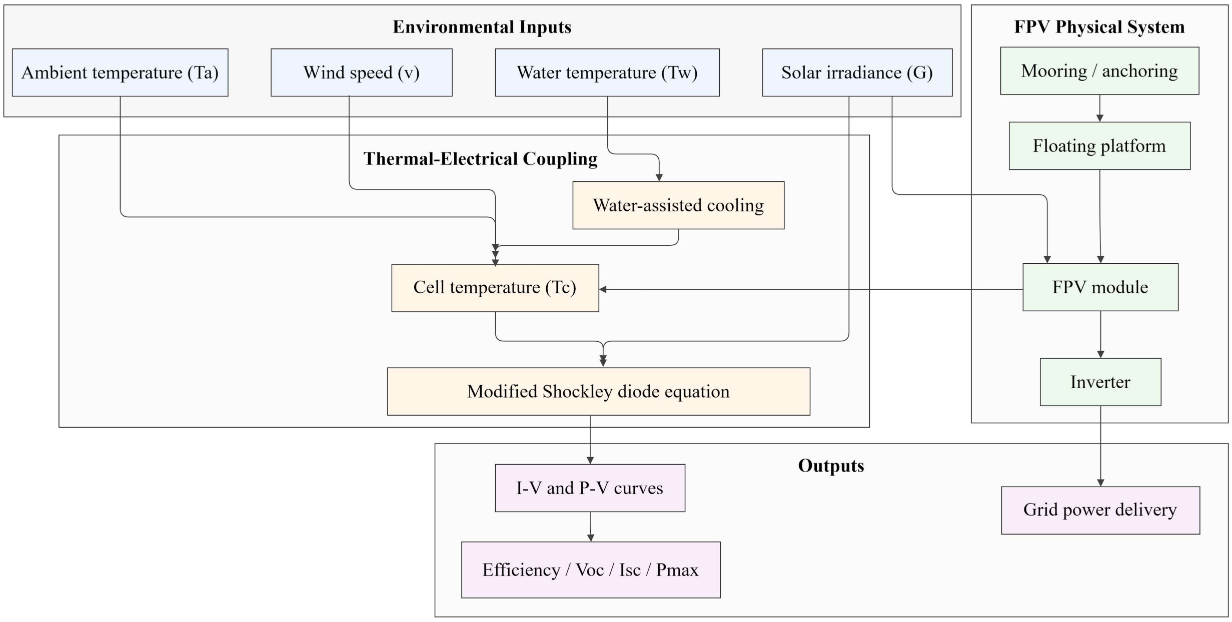

Fig. 1. Block diagram of the representative FPV system and the proposed electrothermal modeling workflow. The system consists of environmental inputs, an FPV physical subsystem, thermal–electrical coupling through water-assisted cooling, the modified Shockley diode model, and electrical output indicators including I–V/P–V curves, efficiency, V_{oc}, I_{sc}, $P_{\max}$, and grid power delivery.

3.1. Reference system configuration and installation assumptions

It should be noted that the present study is based on a numerical reference system rather than on a physically installed experimental plant. Therefore, no site-specific field installation was used. Instead, representative environmental conditions were selected to emulate a typical freshwater FPV deployment scenario. This approach allows the electrothermal influence of floating deployment to be isolated and compared with a land-based reference configuration under controlled and reproducible conditions.

The modeled FPV system represents a typical freshwater deployment, such as a reservoir or artificial pond, where the PV module is mounted on a floating platform and thermally coupled to the underlying water body. The physical configuration includes the floating platform, mooring or anchoring structure, FPV module, inverter, and grid power delivery stage.

A fixed module tilt angle of $\beta = 10°$ and a south-facing azimuth angle of $\gamma = 0°$ were adopted as the reference installation geometry. In the present formulation, the irradiance input G is treated as the effective plane-of-array irradiance incident on the module surface. Therefore, the tilt angle affects the model indirectly through the irradiance input rather than appearing explicitly in the Shockley diode equation.

3.2. Computational workflow

The computational implementation follows a structured four-stage procedure to capture the coupled electrothermal behavior of FPV systems. First, environmental inputs — including G, T_a, T_w, and v — are defined. Second, the FPV-adjusted cell temperature is calculated using (8). Third, the I–V characteristics are obtained by solving the modified Shockley and two-diode equations. Finally, electrical performance metrics — such as power output, efficiency, and comparative indicators — are evaluated.

A block diagram of the representative system considered in this study is shown in Fig. 1. The modeled system consists of an FPV module mounted on a floating platform with mooring or anchoring support, followed by an inverter stage for grid power delivery. Environmental inputs are coupled to the electrical model through the cell-temperature calculation, which allows the physical FPV configuration and the modified Shockley model to be evaluated within a unified framework.

3.3. Implementation of the modified Shockley-based electrothermal model

The proposed framework extends the classical Shockley diode formulation by explicitly incorporating electrothermal coupling mechanisms tailored to FPV systems. Unlike conventional approaches, the cell temperature is not treated as an external parameter but is dynamically determined from environmental variables — including solar irradiance, ambient temperature, water temperature, and wind speed — using a thermal model specific to FPV systems. This temperature is then embedded in temperature-dependent electrical parameters, such as the photocurrent and diode saturation current, thereby modifying the I–V characteristics in a physically consistent manner [33].

FPV-specific thermal effects, including water-assisted cooling and enhanced convective heat transfer, are incorporated through an effective heat-loss coefficient [37]. Parasitic resistances (R_s and R_{sh}) are retained to account for internal ohmic and leakage losses, ensuring a realistic representation of the device. In addition, environmental variability is introduced through a stochastic component to capture transient irradiance fluctuations associated with wave-induced motion.

The resulting nonlinear current–voltage equations are solved iteratively under varying operating conditions to determine the electrical response of the system. From the computed I–V characteristics, key performance metrics are extracted, namely the open-circuit voltage (V_{oc}), short-circuit current (I_{sc}), maximum power ($P_{\max}$), and conversion efficiency. Model validation is performed by comparison with reference photovoltaic data, confirming the proposed framework's ability to accurately capture the electrothermal behavior of FPV systems under realistic environmental conditions.

4. Results and discussion

This section presents the main findings obtained from the proposed modified Shockley framework and discusses the electrothermal behavior of FPV systems in comparison to conventional land-based photovoltaic installations. The results are organized around four complementary aspects: the thermal response of the module, the associated variation in conversion efficiency, the resulting I–V and P–V characteristics, and the overall comparative performance of the FPV configuration under representative environmental conditions.

The analysis demonstrates that the floating configuration provides a clear thermal advantage as a result of the cooling effect of the surrounding water body. This reduction in operating temperature directly affects the voltage-dependent electrical response of the photovoltaic module and, consequently, improves $P_{\max}$ and conversion efficiency. In this respect, the results confirm the theoretical expectation established in Sect. 3, namely that water-assisted thermal regulation modifies the effective operating point of the photovoltaic system and shifts it toward a more favorable electrical regime.

To provide an integrated overview of the main electrothermal trends, the proposed modeling framework summarizes the combined behavior of floating and terrestrial photovoltaic systems. The composite representation includes the current–voltage response, the power–voltage response, the efficiency–temperature dependence, and the environmental sensitivity of the FPV system, thereby offering a compact overview of the major performance indicators discussed in the following subsections.

4.1. Thermal response of floating and land-based photovoltaic systems

The thermal behavior of photovoltaic modules plays a decisive role in determining their electrical performance, particularly under high irradiance conditions. In floating photovoltaic systems, the presence of a water body introduces an additional cooling pathway that significantly alters the temperature–efficiency relationship compared with conventional land-based installations. Figure 2 shows this thermal advantage by comparing the rise in irradiance-dependent temperature and the corresponding efficiency trend for the two configurations.

The thermal response of the photovoltaic module constitutes the most important distinguishing feature between floating and land-based configurations. Because floating modules operate in close thermal contact with a water body, the effective heat-loss coefficient increases and the cell temperature remains lower under identical irradiance conditions. This behavior is directly predicted by the FPV-specific temperature correction introduced in (8).

In both cases, the cell temperature increases with irradiance, as expected from the increasing thermal load imposed by absorbed solar energy. However, the FPV curve remains consistently below that of the land-based system over the full irradiance range, confirming that water-assisted cooling effectively suppresses temperature rise. This lower temperature has direct electrical consequences; since the diode saturation current increases exponentially with temperature, the reduction in FPV operating temperature improves voltage retention and shifts the module toward a more favorable electrical operating point.

4.2. Efficiency dependence on cell temperature

The relationship between cell temperature and conversion efficiency is illustrated in Fig. 3. The results show a clear monotonic decrease in efficiency with increasing cell temperature, consistent with the temperature dependence of the open-circuit

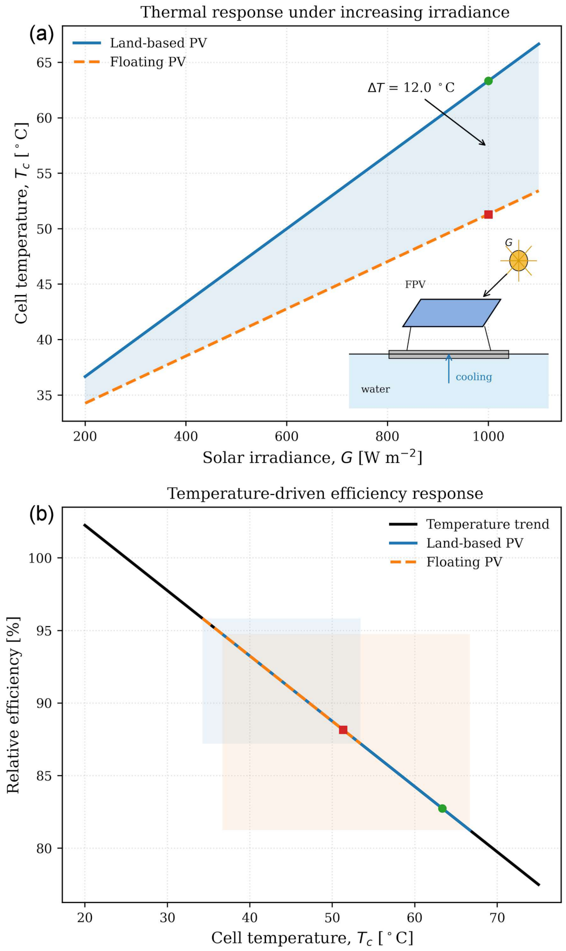

Fig. 2. Thermal-management-oriented comparison between floating and land-based photovoltaic systems. (a) Variation of cell temperature with solar irradiance, showing the reduced thermal rise of FPV modules due to water-assisted cooling, and inset schematic of the cooling mechanism. (b) Relative efficiency response as a function of cell temperature, highlighting the more favorable operating regime of FPV systems under identical environmental loading.

voltage and the saturation current described by (4) and (5). As the module temperature rises, the increase in diode-related losses outweighs the slight gain in short-circuit current, leading to a net reduction in efficiency.

From an FPV perspective, this trend is particularly important because the lower cell temperatures achieved through water-assisted cooling directly translate into improved conversion efficiency. In other words, the thermal advantage of the floating configuration is converted into an electrical benefit through temperature-sensitive diode physics. This result confirms that thermal management is not an auxiliary issue in FPV design, but rather a central determinant of electrical performance. Moreover, the observed efficiency trend supports the

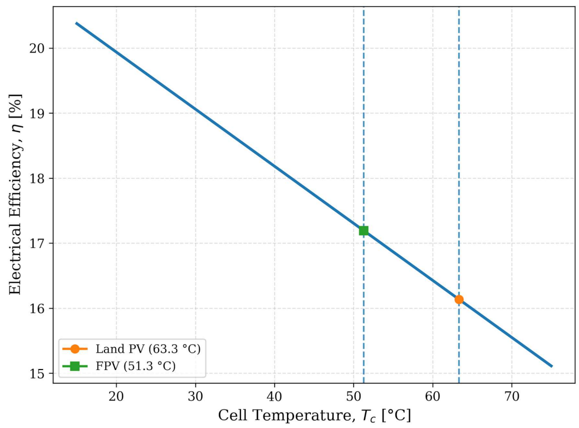

Fig. 3. Variation of photovoltaic conversion efficiency with cell temperature. The decreasing trend highlights the strong temperature sensitivity of photovoltaic performance, emphasizing the advantage of floating photovoltaic systems that operate at lower temperatures due to water-assisted cooling.

validity of the modified Shockley framework, since the model reproduces the expected shift of the operating regime toward higher-efficiency conditions in floating systems.

4.3. Comparative I–V and P–V characteristics

The most direct representation of the electrical differences between floating and land-based systems is provided by the current–voltage and power–voltage characteristics shown in Fig. 4. Under identical irradiance conditions, the FPV system exhibits a higher open-circuit voltage and a slightly higher maximum power point compared to the land-based configuration.

This result is physically consistent with the temperature-dependent behavior of the Shockley model. Because the FPV module operates at a lower temperature, the reverse saturation current remains smaller, allowing the system to preserve a higher voltage over the useful operating range. The current difference between the two configurations is comparatively modest, which is also expected, since the short-circuit current I_{sc} depends much less on temperature than the open-circuit voltage V_{oc}. As a consequence, the main performance gain of the FPV system originates from voltage preservation rather than from a substantial increase in current.

The P–V curves further clarify this point by showing that the floating configuration reaches a higher maximum power point. This indicates that the thermal benefit of the floating system is converted into a measurable electrical advantage in practical operation. In this sense, Fig. 4 provides direct evidence that the proposed thermal correction

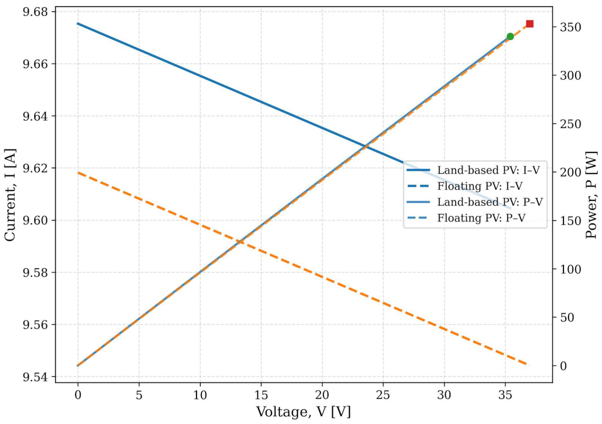

Fig. 4. Comparison of current–voltage (I–V) and power–voltage (P–V) characteristics for floating and land-based photovoltaic systems under identical irradiance conditions. The lower operating temperature of the floating photovoltaic system leads to an increased open-circuit voltage and higher maximum power output.

is not merely theoretical, but has a clear impact on the predicted output characteristics of the photovoltaic module.

4.4. Environmental sensitivity of FPV performance

Figure 5 extends the analysis of the results by identifying the dominant environmental drivers of the FPV performance and classifying the operating parameter space into distinct gain regimes, providing a more design-oriented interpretation of the proposed electrothermal model.

Beyond comparison with land-based systems, the composite results reveal that the FPV performance is also sensitive to variations in water temperature and wind speed. These variables govern the effective heat-loss coefficient of the module and therefore control the FPV-adjusted cell temperature introduced in (8). Lower water temperature and higher wind speed generally increase thermal dissipation, which shifts the operating state toward a lower temperature and improved electrical performance.

This sensitivity analysis highlights an important engineering implication: FPV performance cannot be characterized solely in terms of irradiance, as is often done in simplified photovoltaic studies. Instead, the aquatic thermal environment must be considered an active part of the system. The results therefore support the view that FPV design and performance assessment require an explicitly coupled electrothermal framework capable of accounting for site-specific environmental conditions.

In addition, sensitivity trends help explain why the FPV performance reported in the literature often varies from one installation to another.

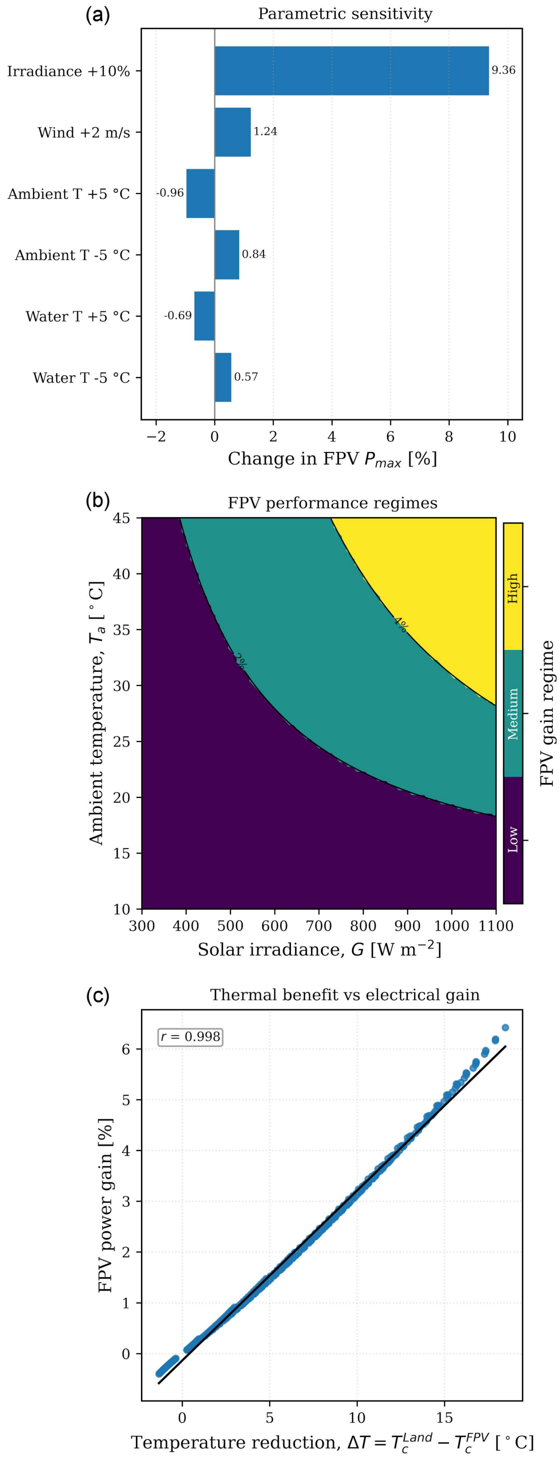

Fig. 5. Parametric sensitivity and performance-regime analysis of FPV systems. (a) Tornado-style sensitivity chart showing the relative change in FPV maximum power under representative environmental perturbations. (b) Performance-regime map classifying FPV gain as low, medium, or high over the irradiance–ambient-temperature parameter space. (c) Relationship between FPV-induced temperature reduction and relative power gain, highlighting the direct electrothermal linkage between thermal regulation and electrical performance.

Differences in wind regime, water temperature, reservoir geometry, and local microclimate can alter the effective cooling capacity of the system and thus influence electrical output. The present model offers a physically interpretable way to capture these variations through a compact set of thermal correction coefficients.

As illustrated in Fig. 6, the proposed electrothermal model reveals a systematic improvement in maximum power output for FPV systems, particularly under elevated thermal loads. This behavior confirms that water-induced cooling shifts the operating regime toward higher-efficiency conditions compared to land-based photovoltaic systems.

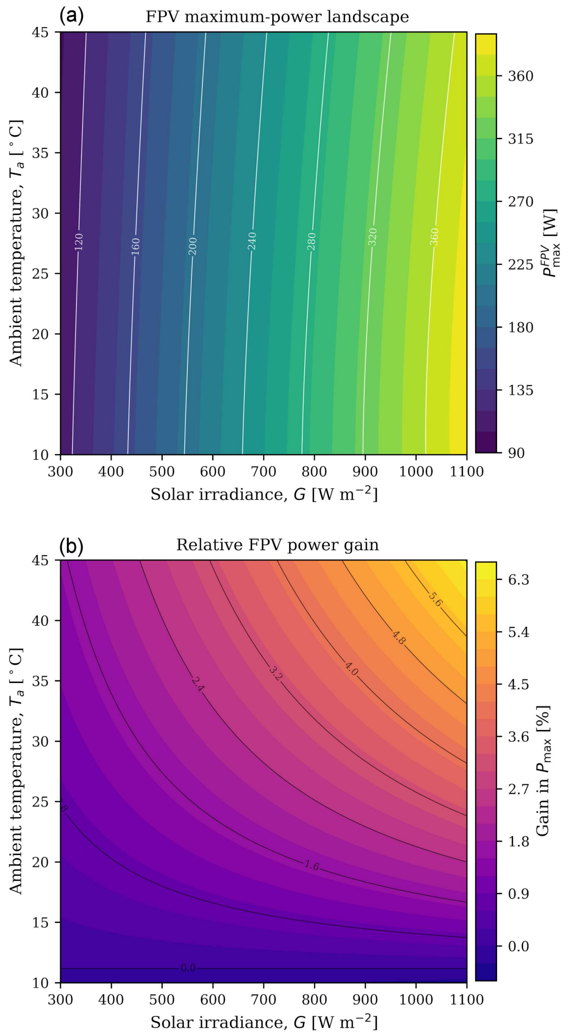

Fig. 6. Results-oriented electrothermal performance maps of FPV systems under varying irradiance and ambient-temperature conditions. (a) Maximum output power predicted for the FPV configuration, with land-based reference contours superimposed for comparison. (b) Relative gain in maximum power of FPV over land-based photovoltaic systems, highlighting the increasing advantage of floating systems under thermally demanding operating conditions.

4.5. Discussion of model validity and physical implications

Figure 7 extends the deterministic analysis by evaluating the robustness of FPV performance under uncertain environmental conditions. The Monte Carlo results show that the floating configuration maintains a statistically consistent power advantage, while the scatter relation confirms that larger temperature reductions are directly associated with stronger electrical gains.

The results obtained from the modified Shockley framework are consistent with the established photovoltaic theory and the expected thermal behavior of floating systems. Lower operating temperatures lead to reduced saturation current, improved voltage retention, and increased maximum power output, confirming the physical validity of the proposed electrothermal coupling.

Although the model captures the dominant thermal–electrical interactions, it remains a simplified representation of FPV operation. Additional factors such as non-uniform irradiance, spectral variability, and hydrodynamic effects may further influence long-term performance. Nevertheless, the strength of the approach lies in its balance between physical interpretability and computational efficiency. Compared with purely empirical models, it preserves a clear physical meaning while remaining sufficiently compact for parametric analysis and system-level optimization.

4.6. Overall comparative performance of FPV systems

Together, the results indicate that floating photovoltaic systems offer a measurable electrical advantage over land-based systems, primarily because of improved thermal regulation. The most important improvement is associated with reduced cell temperature, which leads to a more favorable voltage response and, consequently, higher power conversion efficiency and maximum power output.

These results confirm that the performance benefit of FPV systems is fundamentally electrothermal in nature. The water body does not simply provide a structural support surface — it acts as an active thermal boundary condition that modifies the internal electrical behavior of the photovoltaic module. Consequently, an accurate assessment of FPV systems requires models that explicitly integrate thermal and electrical processes rather than treating temperature as an external or secondary variable.

Overall, the comparative analysis presented in this section supports the validity of the proposed modified Shockley approach and demonstrates its suitability for evaluating FPV systems

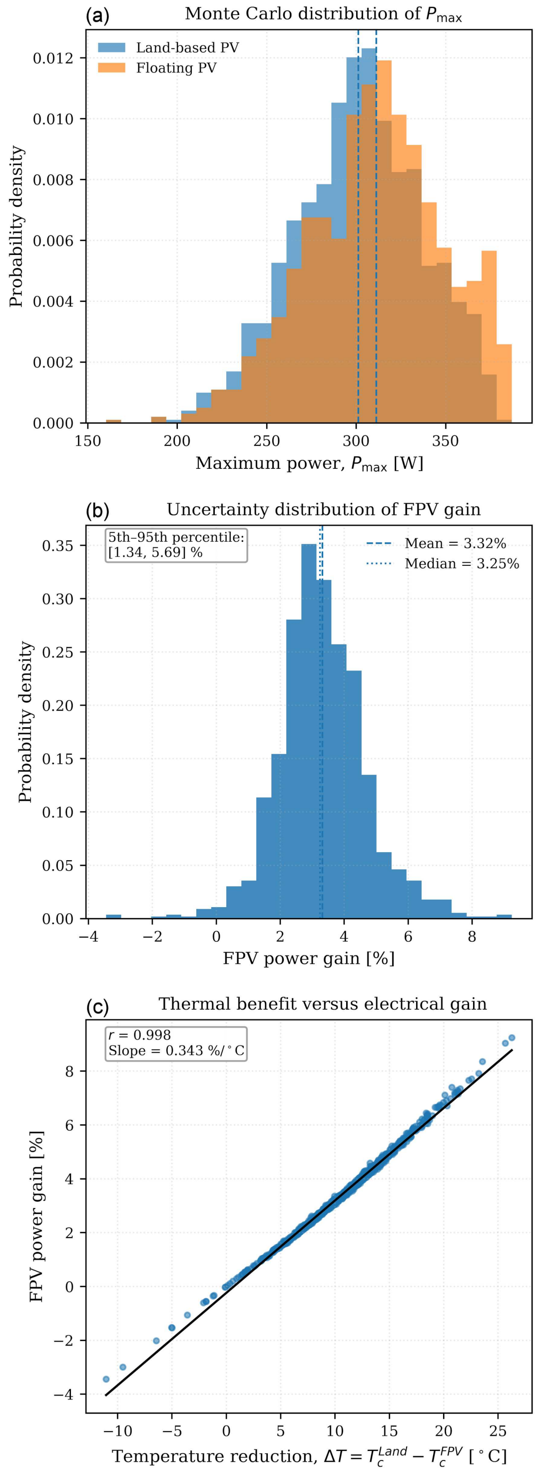

Fig. 7. Monte Carlo uncertainty analysis of floating photovoltaic performance under uncertain environmental conditions. (a) Probability-density distributions of maximum power for floating and land-based photovoltaic systems. (b) Probability-density distribution of the relative FPV power gain, showing the statistical robustness of the floating-system advantage. (c) Relationship between FPV-induced temperature reduction and electrical power gain, confirming the direct electrothermal linkage between thermal regulation and performance improvement.

under variable environmental conditions. The results provide a coherent bridge between theory, modeling, and practical performance interpretation and establish a solid foundation for future experimental validation and site-specific optimization studies.

5. Conclusions

This study presents a physics-based electrothermal framework for analysing FPV systems by extending the classical Shockley diode model to explicitly incorporate water-assisted thermal effects. The proposed formulation establishes a direct coupling between environmental variables and temperature-dependent electrical parameters, enabling a physically consistent interpretation of FPV performance under realistic operating conditions.

The results demonstrate that the primary performance advantage of FPV systems originates from enhanced thermal regulation. Reduced operating temperatures suppress the exponential increase in the diode saturation current, leading to improved voltage retention and higher maximum power output. Consequently, the performance gain is predominantly voltage-driven, while the short-circuit current exhibits only minor sensitivity to temperature variations. Comparative analyses confirm that floating systems operate in a more favorable electrothermal regime than land-based installations.

In addition, environmental factors such as water temperature and wind speed have been shown to play a critical role in determining system performance by influencing the effective heat-loss coefficient and the resulting cell temperature. This highlights the need to explicitly account for aquatic thermal conditions in FPV performance modeling and system design.

Overall, the proposed framework provides a compact, physically interpretable, and computationally efficient tool for evaluating FPV systems. It offers a robust foundation for performance prediction, system optimization, and site-specific assessment, while also enabling straightforward extension toward more advanced multiphysics and experimental validation studies.

References

[1] A. Aouragh, F. Selloum, S. Djeffal, T. Bouarroudj, C. Shekhar, S. Maamri, B. Zaidi, *Acta Phys. Pol. A* **145**, 242 (2024).

[2] C.B. Maia, A. Sônia, A.C. Diniz, S.A. Bonfim, L.L. Kazmerski, *Renew. Energy Environ. Sustain.* **9**, 5 (2024).

[3] M.R.A. Refaai, L. Dhanesh, B.P. Ganthia, M. Mohanty, R. Subbiah, E.M. Anbese, *Int. J. Photoenergy* **2022**, 3891881 (2022).

[4] K. Anusuya, K. Vijayakumar, *Clean. Energy Syst.* **9**, 100140 (2024).

[5] D. Paul, D. Devaprakasam, S. Patil, A. Agrawal, *Int. J. Sustain. Dev. Plan.* **18**, 3213 (2023).

[6] B. Sutanto, H. Iacovides, A. Nasser, A. Cioncolini, I. Afgan, Y.S. Indartono, T. Prasetyo, A.T. Wijayanta, *Appl. Therm. Eng.* **236**, 121801 (2024).

[7] A. Kaul, N. Nobelen, S. Golroodbari, W.G.J.H.M. van Sark, *Solar RRL* **10**, 202500588 (2026).

[8] S.-M. Kim, M. Oh, H.-D. Park, *Appl. Sci.* **9**, 395 (2019).

[9] R. Cazzaniga, M. Cicu, M. Rosa-Clot, P. Rosa-Clot, G.M. Tina, C. Ventura, *Renew. Sustain. Energy Rev.* **81**, 1730 (2018).

[10] M. Hasan, B. Sutrisno, Hartadhi, A. Faradilla, Tarno, B. Kamil, D. Khairiani, N.M. Lande, Y.P. Sibagariang, T.B. Sitorus, *Res. Eng.* **29**, 108791 (2026).

[11] G. Chowdhury, M. Haggag, J. Poortmans, *EPJ Photovolt.* **14**, 24 (2023).

[12] A. Majumder, A. Kumar, R. Innamorati, C.C. Mastino, G. Cappellini, R. Baccoli, G. Gatto, *Energies* **16**, 7939 (2023).

[13] K. Ilgen, D. Schindler, S. Wieland, J. Lange, *Sci. Rep.* **13**, 7932 (2023).

[14] D. Du, J. Darkwa, G. Kokogiannakis, *Solar Energy* **97**, 238 (2013).

[15] H.-P. Wu, C.-Y. Tseng, C.-C. Jen, Y.-C. Chiang, S.-L. Chen, *J. Mar. Sci. Technol.-Taiwan* **32**, 7 (2024).

[16] K.S. Hayibo, M.S. Thesis, Michigan Technological University, 2021.

[17] E. Cuce, P.M. Cuce, S. Saboor, A. Ghosh, Y. Sheikhnejad, *Sustainability* **14**, 2626 (2022).

[18] N.M. Kumar, S. Islam, A.K. Podder, A. Selim, M. Bajaj, S. Kamel, *Front. Energy Res.* **11**, 1075384 (2023).

[19] A. Majumder, R. Innamorati, A. Frattolillo, A. Kumar, G. Gatto, *Energies* **14**, 8336 (2021).

[20] A. Labiod, A. Khadir, *Acta Phys. Pol. A* **147**, 21 (2025).

[21] H. Nisar, A.K. Janjua, H. Hafeez, S. Shakir, N. Shahzad, A. Waqas, *Solar Energy* **241**, 231 (2022).

[22] P. Singh, N.M. Ravindra, *Solar Energy Mater. Solar Cells* **101**, 36 (2012).

[23] L. Essak, A. Ghosh, *Clean Technol.* **4**, 752 (2022).

[24] M. Kumar, H.M. Niyaz, R. Gupta, *Solar Energy Mater. Solar Cells* **233**, 111408 (2021).

[25] V. Nazerian, H. Asadollahi, T. Sutikno, *Int. J. Electr. Comput. Eng. (IJECE)* **13**, 5986 (2023).

[26] A. Karafil, H. Ozbay, M. Kesler, *J. New Results Sci.* **5**, 48 (2016).

[27] A. Ahmed, D. Mahmood, Z. Alqaisi, *Acta Phys. Pol. A* **128**, 461 (2015).

[28] W.C.L. Kamuyu, J.R. Lim, C.S. Won, H.K. Ahn, *Energies* **11**, 447 (2018).

[29] L.H. Slooff, E.E. Bende, A.R. Burgers, T. Budel, M. Pravettoni, R.P. Kenny, E.D. Dunlop, A. Büchtemann, *Rapid Res. Lett.* **2**, 257 (2008).

[30] E. Enasel, A.-G. Lupu, G. Dumitrascu, *Bull. Inst. Polit. Iasi Sect. Mach. Constr.* **69**, 71 (2023).

[31] E. Cuce, P.M. Cuce, I.H. Karakas, T. Bali, *Energy Convers. Manag.* **146**, 205 (2017).

[32] M. Dörenkämper, S. Villa, J. Kroon, M.M. Jong, *Energies* **17**, 2027 (2024).

[33] W. De Soto, S.A. Klein, W.A. Beckman, *Solar Energy* **80**, 78 (2006).

[34] D.L. King, W.E. Boyson, J.A. Kratochvil, "Photovoltaic Array Performance Model", Technical Report SAND2004-3535, Sandia National Laboratories, Albuquerque (NM) 2004.

[35] E. Skoplaki, J.A. Palyvos, *Renew. Energy* **34**, 23 (2009).

[36] N. Anani, H. Ibrahim, *Energies* **13**, 3226 (2020).

[37] A. Sahu, N. Yadav, K. Sudhakar, *Renew. Sustain. Energy Rev.* **66**, 815 (2016).